J|A|C|S
ARTICLES
Published on Web 04/12/2005

Solid-State Composite Electrolyte LiI/3-Hydroxypropionitrile/ SiO_2 for Dye-Sensitized Solar Cells

Hongxia Wang, Hong Li, Bofei Xue, Zhaoxiang Wang, Qingbo Meng,* and Liquan Chen*

Contribution from the Beijing National Laboratory for Condensed Matter Physics, Institute of Physics, Chinese Academy of Sciences, Beijing 100080, China

Received November 9, 2004; E-mail: qbmeng@aphy.iphy.ac.cn; lqchen@aphy.iphy.ac.cn

Abstract: A new compound, LiI(3-hydroxypropionitrile)$_2$, is reported here. According to its single-crystal structure (*C*2/*c*), this compound has 3-D transporting paths for iodine. Further ab initio calculation shows that the activation energy for diffusion of iodine (0.73 eV) is much lower than that of lithium ion (8.39 eV) within the lattice. Such a mono-ion transport feature is favorable as solid electrolyte to replace conventional volatile organic liquid electrolytes used in dye-sensitized solar cells (DSSC). LiI and 3-hydroxypropionitrile (HPN) can form a series of solid electrolytes. The highest ambient conductivity is 1.4×10^{-3} S/cm achieved for LiI(HPN)$_4$. However, it tends to form large crystallites and leads to poor filling and contact within porous TiO_2 electrodes in DSSC. Such a drawback can be greatly improved by introducing micrometer-sized and nanosized SiO_2 particles into the solid electrolyte. It is helpful not only in enhancing the conductivity but also in improving the interfacial contact greatly. Consequently, the light-to-electricity conversion efficiency of 5.4% of a DSSC using LiI(HPN)$_4$/15 wt % nano-SiO_2 was achieved under AM 1.5 simulated solar light illumination. Due to the low cost, easy fabrication, and relatively high conversion efficiency, the DSSC based on this new solid-state composite electrolyte is promising for practical applications.

1. Introduction

Dye-sensitized solar cells (DSSC) have attracted great attention over the past decade owing to high-energy conversion efficiency and low production cost.[1,2] Above 10% light-to-electricity conversion efficiency has been achieved in a DSSC with an organic liquid based electrolyte containing I_3^-/I^- as the redox couple.[1] However, the leakage and evaporation of the liquid electrolyte caused by the technical difficulty in sealing has been a critical factor for long-term practical operation, especially under elevated temperature. Many efforts have been made to solve this problem, such as the use of polymer electrolytes,[3−6] plastic crystal electrolytes,[7,8] or p-type semiconductors,[9−11] or organic hole conductors to substitute for the liquid electrolyte.[12,13] Nevertheless, light-to-electricity conversion efficiencies (η) of the cells fabricated with these solid-state substitutes were not satisfactory, mainly due to low ionic conductivity of the electrolyte and/or poor electrode/electrolyte interfacial contact.

Recently, we have developed a new solid electrolyte system based on LiI and 3-hydroxypropionitrile (HPN).[14] According to the phase diagram, a compound is formed at the molar ratio of 1:2 (LiI/HPN). The electrolyte composed of LiI and HPN shows a solid range when the molar ratio of LiI/HPN is over 1:4. A maximum room-temperature ionic conductivity (1.4×10^{-3} S/cm) for this series was obtained at LiI/HPN = 1:4 (T_m = 121 °C). However, the conductivity mechanism of the electrolytes was not fully understood at that time. Furthermore, the solid electrolyte tends to form large crystallites at room temperature, leading to poor filling of the electrolyte into the pores of the TiO_2 film and bad interfacial contact between the electrolyte and the electrodes. The reproducibility of the cell performance was not satisfactory.

In this paper, the conductivity mechanism of this series of solid electrolytes is further understood on the basis of single-crystal structure and ab initio calculation. We demonstrate that LiI(HPN)$_2$ is an I^- conductor instead of an I^-/Li^+ mixed ionic

(1) O'Regan, B.; Grätzel, M. *Nature* **1991**, *353*, 737.
(2) (a) Nazeeruddin, M. K.; Kay, A.; Rodicio, I.; Humphry, R.; Muller, E.; Liska, P.; Vlachopoulos, N.; Grätzel, M. *J. Am. Chem. Soc.* **1993**, *115*, 6382. (b) Nazeeruddin, M. K.; Pechy, P.; Renouard, T.; Zekeeruddin, S. M.; Humphry-Baker, R.; Comte, P.; Liska, P.; Covey, L.; Costa, E.; Shklover, V.; Spiccia, L.; Beacon, G. B.; Bignozzi, C. A.; Grätzel, M. *J. Am. Chem. Soc.* **2001**, *123*, 1613.
(3) Cao, F.; Oskam, G.; Searson, P. C. *J. Phys. Chem.* **1995**, *99*, 17071.
(4) Ileperuma, O. A.; Dissanayake, M. A. K. L.; Somasundaram, S. *Electrochim. Acta* **2002**, *47*, 2801.
(5) Ren, Y.; Zhang, Z.; Fang, S.; Yang, M.; Cai, S. *Sol. Energy Mater. Sol. Cells* **2002**, *71*, 253.
(6) Nogueira, A. F.; Paoli, M.-A. De.; Montanari, I.; Monkhouse, R.; Nelson J.; Durrant, J. R. *J. Phys. Chem. B* **2001**, *105*, 7517.
(7) Wang P.; Dai, Q.; Zakeeruddin, S.M.; Forsyth, M.; MacFarlane, D. R.; Gratzel, M. *J. Am. Chem. Soc.* **2004**, *126*, 13590.
(8) Dai, Q.; MacFarlane, D. R.; Howlett, P. C.; Forsyth, M. *Angew. Chem. Int. Ed.* **2005**, *44*, 313.
(9) O'Regan, B.; Schwartz, D. T. *Chem. Mater.* **1995**, *7*, 1349.
(10) Tennakone, K.; Fernando, C. A. N.; Dewasurendra, M. J. *J. Photochem.* **1989**, *38*, 75.
(11) Meng, Q.-B.; Takahashi, K.; Zhang, X.-T.; Sutanto, I.; Rao, T. N.; Sato, O.; Fujishima, A. *Langmuir* **2003**, *19*, 3572.
(12) Bach, U.; Lupo, D.; Comte, P.; Moser, J.-E.; Weissorter, F.; Salbeck, J.; Spreitzer, H.; Grätzel, M. *Nature* **1998**, *395*, 583.
(13) Smestad, G. P.; Spiekermann, S.; Kowalik, J.; Grant, C. D.; Schwartzberg, A. M.; Zhang, J.; Tolbert, L. M.; Moons, E. *Sol. Energy Mater. Sol. Cells* **2003**, *76*, 85.
(14) Wang, H. X.; Xue, B. F.; Hu, Y. S.; Wang, Z. X.; Meng, Q. B.; Huang, X. J.; Chen, L. Q. *Electrochem. Solid-State Lett.* **2004**, *7* (10), A302.

10.1021/ja043268p CCC: $30.25

conductor. This is a suitable solid electrolyte system for DSSC in view of the transport. Moreover, it is found that the addition of micrometer- and nanometer-sized silica into this organic crystal electrolyte can improve their ionic conductivities and hinder the formation of large crystallites effectively. Consequently, the interfacial situation of the DSSC assembled with the composite electrolyte is improved. Benefiting from these two factors, a conversion efficiency of 5.4% was achieved with a DSSC under AM 1.5 simulated solar light illumination (100 mW/cm^2).

2. Experimental Section

2.1. Preparation of the Electrolytes. The electrolytes were prepared by mixing anhydrous LiI (99%, Acros Organics) and 3-hydroxypropionitrile (HPN, 98%, Acros Organics) with the required molar ratio in an argon-filled glovebox (M.Braun), first heating the mixture until a homogeneous melt was obtained and then cooling to room temperature naturally. The electrolytes containing inert oxide additives were prepared by adding the silica powder with controlled content into the above melts, stirring, and ultrasonicating vigorously until a homogeneous composite was formed. Two kinds of silica powder were used as received (micrometer SiO_2 with particle diameter 0.3−2 μm, ultrafine, Tianjin Chemical Reagent Factory, China; nanometer SiO_2, 15 nm, Degussa). The morphology of the electrolytes was investigated by a scanning electron microscope (SEM, Hitachi S-4000).

2.2. Impedance Measurement. The ionic conductivities of the electrolytes were determined by an HP 4192A impedance analyzer from 5 Hz to 13 MHz between 20 and 50 °C in a sealed cell. The test cell has a sandwich structure of "stainless steel/electrolyte/stainless steel" assembled in an argon-filled glovebox. The electrolyte was melted in advance and filled between two electrode plates in order to improve the interfacial contact. The distance between two electrodes is fixed by a special design. The impedance spectra were analyzed with the Zview program.

2.3. X-ray Structure Determination. Single crystals were obtained from a LiI/(HPN) (1:4) cooled melt in the glovebox. A suitable single-crystal particle with dimension of 0.794 × 0.285 × 0.421 mm^3 was selected for X-ray diffraction. The crystal was sealed in a capillary to protect the sample from moisture. The data were collected on a Rigaku R-AXIS RAPID IP diffractometer (λ(Mo Kα) = 0.71073 Å) at 293 ± 2 K. Intensities were corrected for Lorentz−polarization. The structure was solved by direct methods. In all cases all of the non-hydrogen atoms were refined anisotropically by full-matrix least squares based on F^2 using the SHELXTL program. The positions of the hydrogens bonded to oxygen were located by differential Fourier synthesis. Details of the data collection and refinement are summarized in Table 1.

2.4. Photoelectrochemical Measurement. A solar light simulator (Oriel, 91192) was used to give an illumination of 100 mW/cm^2 (AM 1.5) on the surface of the solar cells. The incident light intensity was measured with a radiant power/energy meter (Oriel, 70260) before each experiment. The characteristics of the photocurrent density−photovoltage of the cell under these conditions were recorded by a potentiostat (Princeton Applied Research, Model 263A).

2.5. TiO_2/Dye Film Preparation. The nanocrystalline TiO_2 film was fabricated by a screen-printing technique according to the literature.[15] The TiO_2 (P25) paste was deposited on a conducting glass substrate (F-doped SnO_2, 10 Ω /□), followed by sintering at 450 °C for 30 min. The thickness of the film was about 10 μm. The mesoporous TiO_2 film was preheated at 120 °C for 30 min before it was immersed into a solution of the dye *cis*-dithiocyanate-*N*,*N*′-bis(4,4′-dicarboxylate-2,2′-bipyridine)ruthenium(II) (RuN3, Solaronix) with a concentration of 3 × 10^{-4} M in dry ethanol overnight.

(15) Ma, T.; Kida, T.; Akiyama, M.; Inoue, K.; Tsunematsu, S.; Yao, K.; Noma, H.; Abe, E. *Electrochem. Commun.* **2003**, *5* (4), 369.

Table 1. Crystal Data and Structure Refinement for LiI(HPN)$_2$

chemical formula	LiI(C_3H_5NO)$_2$
fw	276
cryst syst	monoclinic
space group	*C*2/*c*
cryst color	colorless, transparent
lattice params	
a (Å)	14.097(3)
b (Å)	14.036(3)
c (Å)	10.923(2)
β (deg)	99.97(3)
V (Å^3)	2128.6(7)
Z	8
density ρ (g/cm^3)	1.722
absorp coeff μ (mm^{-1})	2.973
F(000)	1056
T (K)	293 ± 2
reflns measd	2417
params refined, N_p	119
refinement method	full-matrix least squares on F^2
final *R* indices [$I > 2\sigma(I)$]	$R_1 = 0.0233$, $wR_2 = 0.0565$
final *R* indices (all data)	$R_1 = 0.0274$, $wR_2 = 0.0576$
goodness-of-fit on F^2	1.075
largest diff peak and hole (e/Å^3)	0.403, −0.449

2.6. Fabrication of the DSSC. The composite electrolytes were first dissolved in a mixture of solvents dimethyl carbonate (DMC) and propylene carbonate (PC) (Battery Grade, 4:1, v/v) and stirred vigorously for 30 min. Then a droplet of the electrolyte solution was dropped onto the surface of the TiO_2 film. The solvents were removed under vacuum conditions. The same procedure was repeated several times until the TiO_2 film was covered with the electrolyte. Finally, an open sandwich-type cell, which was not sealed, was fabricated in air by clamping the TiO_2/electrolyte with a thermally platinized ITO counter electrode with two clips. The active electrode area was 0.15 cm^2.

3. Results and Discussion

3.1. Single-Crystal Structure of LiI(HPN)$_2$. The differential scanning calorimeter (DSC) of LiI(HPN)$_2$ (Figure S1) indicates that only one sharp endothermic peak appears at 142 °C in the temperature range from −80 to 150 °C. This suggests that the compound is a single-phase crystalline material. From the phase diagram of the system LiI/HPN, only one compound exists in this system.[14] Moreover, a transparent crystal was found in a LiI/HPN (1:4 molar ratio) cooled melt in the glovebox and picked out for further measurement.

Single-crystal structure analysis (Table 1) indicates that the molecular formula of the compound is $LiIC_6H_{10}N_2O_2$ (LiI(HPN)$_2$) and the molecular weight is 276. It belongs to the *C*2/*c* space group with the monolithic parameters $a = 14.097(3)$ Å, $b = 14.036(3)$ Å, $c = 10.923(2)$ Å, and $\beta = 99.97(3)°$. There are eight molecules in a unit cell.

According to the crystal structure (Figure 1), one lithium ion is coordinated with four atoms. For example, Li(1) is coordinated with N(1) and N(2) of the nitrile group and O(1A) and O(2B) of the hydroxyl group. Two lithium ions are connected via two HPN molecules to form a closed 12-membered ring. Two neighboring rings show an inclined angle of 91°. The bond lengths of Li(1)−O(1A) and Li(1)−O(2B) are 1.913(4) and 1.918(5) Å, and Li(1)−N(1) and Li(1)−N(2) are 2.028(4) and 2.027(4) Å, respectively. It is known that the bond lengths of Li−O and Li−N in inorganic compounds are in the range of 1.9−2.1 and 1.94−2.3 Å, respectively.[16] The above data indicate that strong chemical bonds between Li and O and N atoms exist in the LiI(HPN)$_2$ compound.

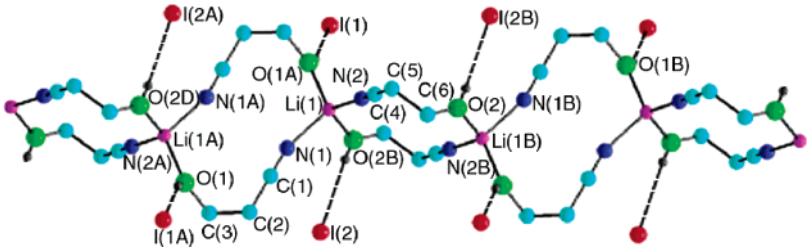

Figure 1. X-ray structure of LiI $(HPN)_2$.

Table 2. Bond Lengths and Angles of Hydrogen Bonds for $LiI(HPN)_2$[a]

O–H···I	d_{O-H} (Å)	$d_{H\cdots I}$ (Å)	$d_{O\cdots I}$ (Å)	bond angle (deg)
O(1)−H(1A)···I(1)#1	0.73(3)	2.68(3)	3.387(6)	163(3)
O(2)−H(2C)···I(2)#2	0.73(2)	2.74(2)	3.458(7)	169(3)

[a] Symmetry transformation used to generate equivalent atoms: #1 $-x-1/2, -y-1/2, -z+2$; #2 $-x-1/2, -y-1/2, -z+1$

The hydrogen bond lengths and angles between I···HO for the compound are listed in Table 2. The bond length of H(1A)···I(1) is 2.68(3) Å, and H(2C)···I(2) is 2.74(2) Å. Details of other bond lengths, bond angles, and atomic coordinates for the single-crystal structure are listed in the Supporting Information (Tables S1, S2).

Figure 2 shows the structure plots for $LiI(HPN)_2$ along the *a*, *b*, and *c* axis, respectively. The hydrogen bond is omitted for clarity. It can be seen clearly that lithium atoms (green balls) are coordinated with O and N atoms, and 3-D diffusion tunnels for iodine atoms (pink balls) are available in view of the geometry structure. This is an interesting result since fast diffusion of I^- anions is important for mass transport in the electrolyte and guarantees the efficient regeneration of the oxidized dye in the DSSC. In addition, it is found that the photovoltage of DSSC is in proportion to the ionic radius of the cations of the electrolyte.[17,18] The trapping of Li ions is favorable.

It is worthy to determine whether this compound is a unique I ion conductor or Li ion conductor or a mixed conductor. In principle, we performed ab initio density functional based total energy calculations using the Vienna VASP software package under local density approximation (LDA). After structure optimization, a so-called "adiabatic trajectory method"[19,20] was applied to calculate the diffusion barriers of ions along different paths. The results indicate that the activation energy for the hopping of I^- to its neighboring sites along the *c* direction shows a lower value (0.73 eV) than that of Li^+ (8.39 eV). This suggests that lithium is immobile and this compound is an iodine conductor. The details of the theoretical calculations will be reported later by Shi, Xu and Wang.

In experiment, however, it is difficult to use ion-block-based electrochemical techniques to measure the diffusion coefficient of Li^+ and I^- and compare them quantitatively because the electrolyte is reactive to metallic lithium and a pure iodine ion conductor is not available right now. Therefore, a special experiment was performed and the result showed qualitatively that only the I^- ion was mobile. The details can be found in the Supporting Information. Determination of the unique I^- transport feature in this solid electrolyte quantitatively needs further confirmation by other techniques, such as ^7Li and ^{127}I solid NMR.

3.2. Influence of Silica on the Conductivity of the Electrolyte. For a homogeneous electrolyte system, ionic conductivity is proportional to the free ion concentration (*c*) and its mobility (μ) ($\sigma = zecu$). As for $LiI(HPN)_x$ composites, FTIR spectra indicate that the interaction between LiI and HPN occurs at very low lithium salt content (LiI/HPN = 1:100).[14] The conductivity increases with increasing LiI concentration due to enhanced concentration of free ions. A maximum conductivity at room temperature was obtained at LiI/HPN = 1:15 ($\sigma = 6.8 \times 10^{-3}$ S/cm). Beyond the limitation, further adding LiI leads to enhanced concentration of associated ionic pairs and the conductivity decreases gradually. When the ratio of LiI to HPN reaches 1:4, solid electrolyte is formed. Moreover, for the solid electrolyte $LiI(HPN)_2$, all Li^+ ions are coordinated by N and O atoms and cannot move; only I^- ions can diffuse as mentioned above. Therefore, ionic conductivity should be contributed mainly from I^- diffusion in bulk phase along 3-D paths. As for the solid-state electrolyte $LiI(HPN)_x$ in the range of $2 \le x \le 4$, the highest conductivity was found for the sample $LiI(HPN)_4$.[21]

From the phase diagram of the system LiI/HPN,[14] we suppose that $LiI(HPN)_4$ should be a solid composed of $LiI(HPN)_2$ and 2 HPN molecules. The local crystal structure is not clear now. However, it is safe to state that the existence of extra HPN in the electrolyte should introduce a large number of interfacial areas and vacancies for iodine transport, leading to the enhancement of the ionic conductivity.

The determination of the single-crystal structure of $LiI(HPN)_2$ is helpful for us to understand the transport mechanism. In view of practical application, $LiI(HPN)_4$ shows the highest ionic conductivity among this series of solid electrolytes. Therefore, this system is investigated preferentially.

For a heterogeneous or nanostructured system, ionic conductivity is contributed from both bulk and interfacial transport. Interfacial contribution becomes even more important in many cases. It is well-known that addition of ceramic oxide into either ionic conductive salts (MX) or polymer/salt electrolytes can increase their ionic conductivities significantly.[22,23] The enhancement mechanism is attributed to the increasing of the

(16) (a) Foeppl, H. *Z. Anorg. Allg. Chem.* **1957**, *291*, 12. (b) Zintl, E.; Harder, A.; Dauth, B. *Trans. J. Br. Ceram. Soc.* **1983**, *83*, 32. (c) Schulz, H.; Thiemann, K. H. *Acta Crystallogr. B* **1982**, *24*, 1968. (d) Gregory, D. H.; O'Mears, P. M.; Gordon, A. G.; Hodges, J. P.; Short, S.; Jorgensen, J. D. *Chem. Mater.* **2002**, *14*, 2063.
(17) Liu, Y.; Hagfeldt, A.; Xiao, X. R.; Linquist, S. E. *Sol. Energy Mater. Sol. Cells* **1998**, *55*, 267.
(18) Hara, K.; Horiguchi, T. Kinoshita, T.; Sayama, K.; Arakawa, H. *Sol. Energy Mater. Sol. Cells.* **2001**, *70*, 151.
(19) Wang, C.; Zhang, Q. M.; Bernholic, J. *Phys. Rev. Lett.* **1992**, *69*, 3789.
(20) Zhang, Q. M.; Roland, C.; Boguslawskiand, P.; Bernholic, J. *Phys. Rev. Lett.* **1995**, *75*, 101.
(21) Wang, H.; Wang, Z.; Xue, B.; Meng, Q.; Huang, X.; Chen, L. *Chem. Commun.* **2004**, 2186.
(22) Liang, C. C. *J. Electrochem. Soc.* **1973**, *120*, 1289.
(23) Ji, K.-S.; Moon, H.-S.; Kim, J.-W.; Park, J.-W. *J. Power Sources* **2003**, *117*, 124.

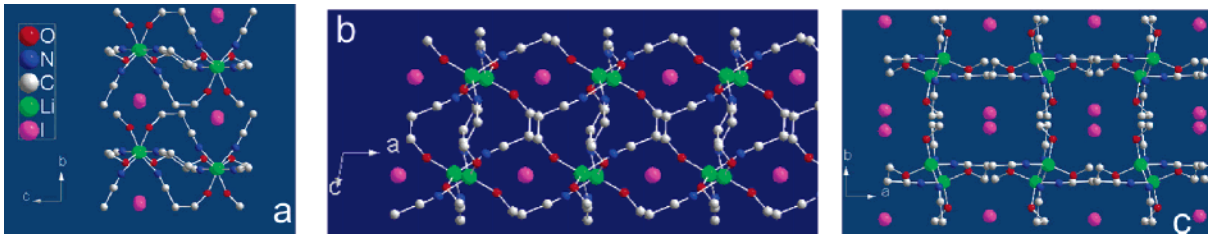

Figure 2. X-ray structure plot for the compound viewed along the *a*, *b*, and *c* axes.

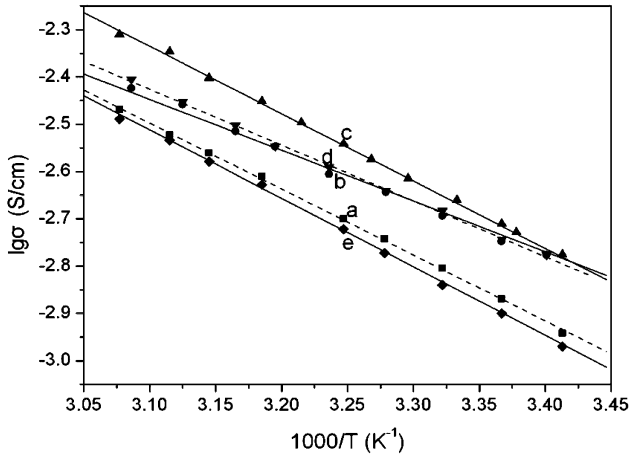

Figure 3. Arrhenius plots, representing the temperature dependence of the ionic conductivity of different electrolyte compositions. (a) LiI/HPN = 1:4 (molar ratio) without SiO_2 (dashed line); (b) 15 wt % SiO_2 (solid line); (c) 20 wt % SiO_2 (solid line), (d) 25 wt % SiO_2 (dashed line); (e) 30 wt % SiO_2 (solid line). Particle size of silica: 0.3−2 μm.

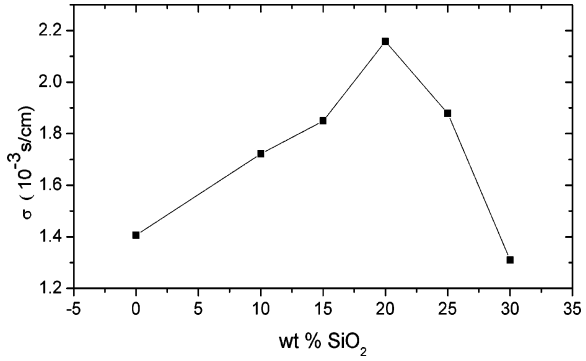

Figure 4. Variation of ambient conductivity of the electrolytes versus weight ratio of silica (0.3−2 μm) in LiI/HPN (1:4).

interfacial defect concentration due to the space charge layer effect in the case of the MX/oxide system,[22,24] or the inhibiting of the crystallization of polymer electrolyte,[23,25] and/or promoting the dissociation of lithium salts in polymer systems.[26,27] Recently, such an enhancement effect was observed even in the liquid electrolyte $LiClO_4$/methnol/SiO_2 due to the promoting-dissociation of the ionic pair by surface interaction of silica and the Li salt.[28] Herein, the same strategy is applied in the $LiI(HPN)_4$ electrolyte.

An enhancement of the conductivity was observed when silica (size: diameter = 0.3−2 μm) was introduced into the electrolyte. The temperature dependence of the ionic conductivity for the $LiI(HPN)_4/SiO_2$ (particle size: 0.3−2 μm) composite electrolyte is shown in Figure 3. All samples show Arrhenius behavior in the observed temperature range instead of a VTF response in the case of the polymer system.[24] Figure 4 displays the ionic conductivities of this system as a function of SiO_2 content ($W_{SiO2}/W_{(LiI+HPN)}$) at 25 °C. The conductivity of the electrolyte initially increases with increasing SiO_2 content. At wt % = 20 SiO_2 (0.3−2 μm), a maximum room-temperature conductivity of $\sim 2.1 \times 10^{-3}$ S/cm is achieved. As the SiO_2 content is further increased, the conductivity decreases. For the composite electrolyte containing 30 wt % SiO_2, the conductivity is even lower than that of the electrolyte without SiO_2. The dependence of conductivity on the silica content obeys a percolation type of conductivity behavior, as in MX/oxide cases.[24]

Figure 5a,b compares the morphology of $LiI(HPN)_4$ electrolyte with and without SiO_2 additive. The $LiI(HPN)_4$ sample tends to form very large crystallites at room temperature (Figure 5a, average size: 400 μm). After adding micrometer-sized silica into the electrolyte, the sample appears as many small agglomerates composed of tiny particles (Figure 5b, average size < 40 μm), indicating that the crystallization process was hindered significantly.

The conductivity behaviors of $LiI(HPN)/\mu m\text{-}SiO_2$ obey an Arrhenius response instead of the VTF equation. Therefore, the conductivity enhancement cannot be related to the formation of a bulk amorphous conductive organic phase as significantly as in the cases of polymer electrolytes (XRD data, see Figure S2). Actually, the addition of silica introduces the interfacial regions between $LiI(HPN)_4$ and silica. This should be a typical example of interfacial conductivity enhancement, very similar to the case of oxide filler added into an inorganic conductive salt.[22]

The interfacial conductivity enhancement mechanism is related to the surface interaction between the oxide filler and the conductive phase. It leads to dissociation of ionic pairs and an increase of the concentration of either anions or cations at the interfacial region, depending on the polarity of the oxide surface.[24] The surface ζ-potential measurement for the used $\mu m\text{-}SiO_2$ shows a value of −22 mV in distilled water. Acidic SiO_2 surface (pH of zero charge (pzc) $\approx$ 2−3[29,30]) tends to absorb anions and reduce the association between the cations and anions.[28] It can enhance the conductivity of cations in cases where the cations are more mobile. As mentioned above, for the $LiI(HPN)_4$ system, Li^+ ions are strongly coordinated by O and N atoms. Only I^- ions are mobile in the crystal lattice.

(24) Maier, J. *Prog. Solid State Chem.* **1995**, *23*, 171.
(25) Croce, F.; Appetecchi, G. B.; Persi, L.; Scrosati, B. *Nature* **1998**, *394*, 456.
(26) Wang, Z.; Huang, X.; Chen, L. *Electrochem. Solid-State Lett.* **2003**, *6*, E40.
(27) Byrne, N.; Efthimiadis, J.; MacFarlane, D. R.; Forsyth, M. *J. Mater. Chem.* **2004**, *14*, 127.
(28) Bhattacharyya, A. J.; Maier, J. *Adv. Mater.* **2004**, *16*, 811.
(29) Reed, J. S. In *Principle of Ceramics Processing*, 2nd ed.; John Wiley & Sons: New York, 1995; p 152.
(30) Palomares, E.; Clifford, J. N.; Haque, S. A.; Lutz, T.; Durrent, J. R. *J. Am. Chem. Soc.* **2003**, *125*, 475.

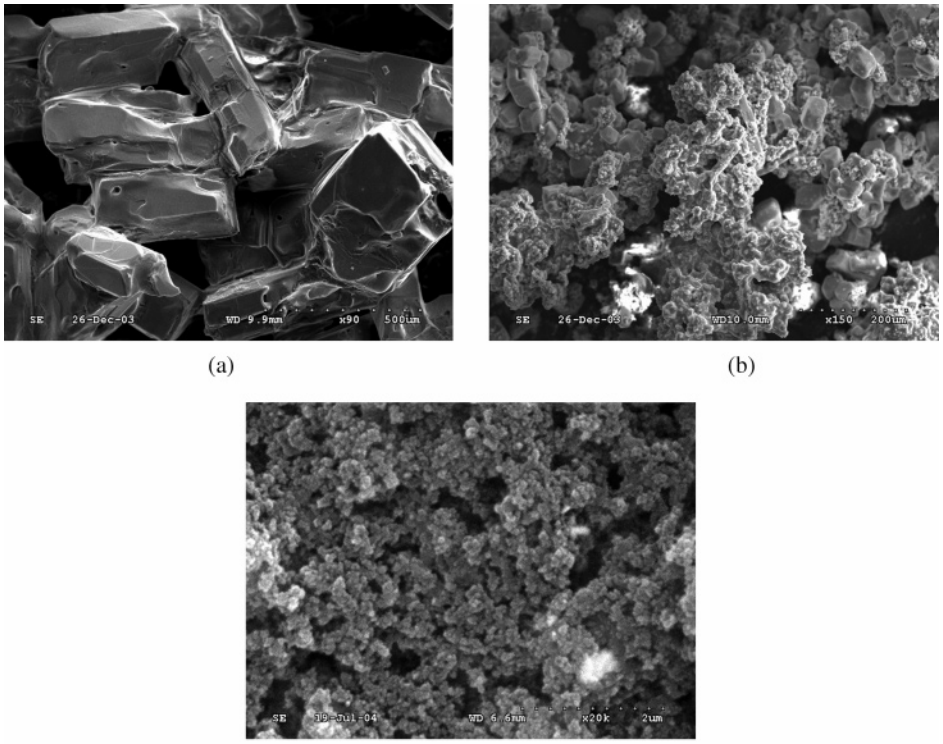

Figure 5. (a) SEM image of LiI/HPN (1:4) without SiO_2, (b) SEM of LiI/HPN (1:4) containing 20 wt % μm-SiO_2 (0.3−2 μm), and (c) SEM of $LiI(HPN)_4$ containing 15 wt % nano-SiO_2 (15 nm).

Therefore, the surface interaction between SiO_2 and $LiI(HPN)_4$ will increase the concentration of I^- at the interfacial regions. On the other hand, it is plausible that the contact and the interaction between oxide filler and lithium salts will lead to the formation of amorphous regions at the $SiO_2/LiI(HPN)_4$ interfacial area. I^- ions could be more mobile at the interfacial regions than those in the bulk lattice of $LiI(HPN)_4$. This should be the reason for conductivity enhancement.

As discussed above, the conductivity enhancement mechanism is related to interfacial interaction. Nanosized SiO_2 possesses a larger surface area and should be more effective for this purpose. The room-temperature conductivity (2.1×10^{-3} S/cm) of 5 wt % nano-SiO_2 ($\zeta_{potential} = -15$ mV) in the $LiI(HPN)_4$ electrolyte has roughly the same value as that of 20 wt % μm-SiO_2 in the electrolyte due to its small tap density and large surface/volume ratio. The maximum conductivity (2.5×10^{-3} S/cm) is achieved at the composition of the electrolyte containing a lower weight ratio of nano-SiO_2 (3 wt %). However, in view of decreasing the particle size and increasing interfacial regions, more nano-SiO_2 is more effective. Figure 5c shows the SEM image of $LiI(HPN)_4$/15 wt % SiO_2 (15 nm). It can be seen that the crystallization of $LiI(HPN)_4$ is further hindered, more homogeneous composite is formed, and the average particle size decreases to less than 100 nm. However, the room-temperature conductivity decreases to 1.3×10^{-3} S/cm for the electrolyte $LiI(HPN)_4$−15 wt % SiO_2 (15 nm) due to too much nonconductive filler.

3.3. Effect of μm-SiO_2 on the Performance of DSSC. Figure 6 shows the $I-V$ curve of DSSC assembled using electrolytes with and without silica (20 wt % μm-SiO_2). Obviously, the performance of the DSSC is greatly improved when silica is added into the electrolyte. The conversion efficiency is increased from 1.4% for $LiI(HPN)_4$ to 3.6% for $LiI(HPN)_4$/20 wt % μm-SiO_2.

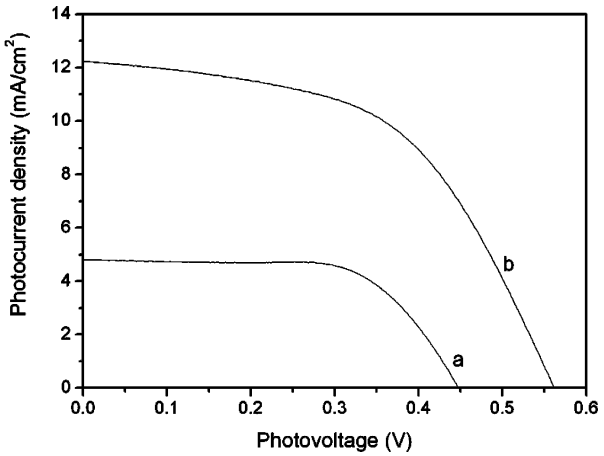

Figure 6. Photocurrent−voltage characteristics of DSSC fabricated with $LiI(HPN)_4$ (a) and $LiI(HPN)_4$/20 wt % SiO_2 (0.3−2 μm) (b) electrolytes under AM 1.5 illumination (100 mW/cm^2).

Moreover, it is found that the open-circuit voltage (V_{oc}), short-circuit photocurrent density (J_{sc}), and light-to-electricity conversion efficiency (η) of the DSSC (Figure 7(a,b,c)) show consistent variation with the content of silica, especially consistent with the conductivity variation as in Figure 7d (redrawn from Figure 4 for convenience).

Photoelectricity conversion processes of DSSC are mainly related to electron injection at the TiO_2/dye interface and hole transfer at the dye/electrolyte interface, in addition to the transport of I^-/I_3^- in bulk electrolyte phase and pores of the TiO_2 electrode. It is reasonable that the high conductivity of the I^-/I_3^- couple is favorable to achieve high J_{sc}, as clearly

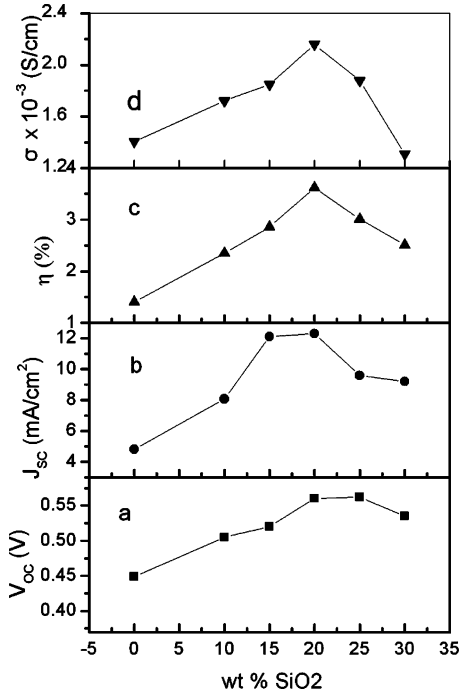

Figure 7. Dependence of J_{sc}, V_{oc}, and η of DSSC assembled with LiI-$(HPN)_4$/μm SiO_2 (0.3−2 μm) on the content of silica in the electrolyte. The radiant power is 100 mW/cm^2 (AM 1.5).

evidenced in Figure 7b,d. On the other hand, according to Figure 5, addition of silica hinders the crystal growth of LiI$(HPN)_4$. LiI$(HPN)_4$ tends to form big crystals on the surface of the TiO_2 mesoporous film (see Figure S3(a)). By introducing silica, the crystallization of the solid electrolyte was restrained significantly. Uniform composite electrolyte LiI$(HPN)_4$/20 wt % SiO_2 (0.3−2 μm) with smaller particle size was formed on the surface of the TiO_2 film (see Figure S3(b)). Therefore, the filling of solid electrolyte within the porous structure of the TiO_2 electrode and the electrolyte/electrode contact are improved significantly, which is also important for interfacial charge transfer.

A power-law experiment of DSSC is always carried out to evaluate whether J_{sc} is controlled by the diffusion of I^-/I_3^- in nanocrystalline TiO_2 films. A linear response of J_{sc} versus radiant power indicates that the photocurrent is not limited by mass transport.[2a] Figure 8 illustrates the relationship of J_{sc} of DSSC fabricated with several solid electrolytes versus radiant power. It can be seen that DSSC using LiI$(HPN)_4$ as electrolyte shows a nonlinear response and J_{sc} reaches a saturated value under higher power radiation (Figure 8a), while the J_{sc} of LiI$(HPN)_4$/20 wt %-SiO_2(μm) and LiI$(HPN)_4$/15 wt %-nano-SiO_2 shows a nearly linear response to radiant power (Figure 8b,c).

It should be pointed out that these electrolytes do not contain iodine in advance. I_3^- is formed spontaneously at the TiO_2/electrolyte interfacial region after irradiation. This has been confirmed by UV−vis spectroscopy (not shown) that absorption peaks at 290 and 360 nm were observed, a feature of the absorption of I_3^-.[31] This demonstrates that a trace amount of I_3^- was formed during the operation of the DSSC. Presuming the system reaches the steady state and the reaction rate of electron transfer is not related to the electrolyte, the concentration of I_3^- at the TiO_2/electrolyte interfacial region is determined

(31) Popov, A.; Swemsem, R. F. *J. Am. Chem. Soc*. **1955**, *77*, 3724.

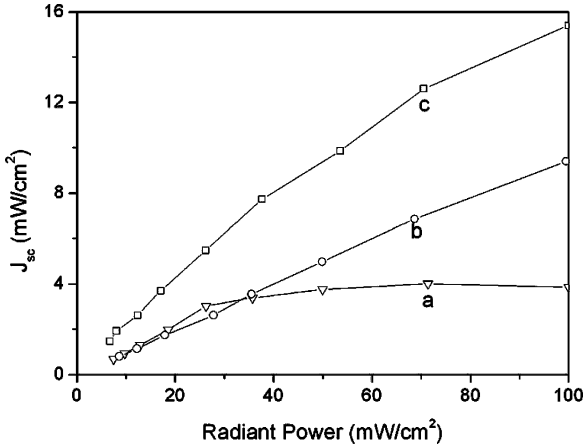

Figure 8. J_{sc} versus radiation power for DSSC using different solid electrolyte: (a) LiI$(HPN)_4$, (b) LiI$(HPN)_4$/20 wt % μm-SiO_2, (c) LiI$(HPN)_4$/15 wt % nm-SiO_2.

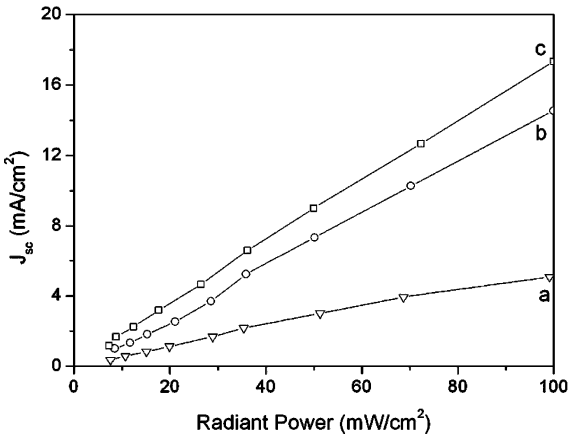

Figure 9. J_{sc} versus radiation power for DSSC using different solid electrolyte containing I_2 (I_2/LiI = 1:50): (a) LiI$(HPN)_4$, (b) LiI$(HPN)_4$/20 wt % μm-SiO_2, (c) LiI$(HPN)_4$/15 wt % nm-SiO_2.

by the diffusion of I^- from the counter electrode to the TiO_2 electrode and the formation rate of I_3^- by oxidation of I^- ($3I^- - 2e^- \rightarrow I_3^-$). Obviously, high J_{sc} needs fast diffusion of I^- and I_3^-. Comparing parts a and b of Figure 8 with part c, it seems that the solid/electrolyte system with higher ionic conductivity can achieve higher J_{sc}. However, the ionic conductivity of LiI$(HPN)_4$/15 wt % nano-SiO_2 is 1.3×10^{-3} S/cm, but it shows the highest J_{sc} value. As we mentioned above, J_{sc} is also related to interfacial electron transfer at electrode/electrolyte. LiI$(HPN)_4$/15 wt % nano-SiO_2 has much better interfacial contact and a better filling ratio compared to the other two systems. It is believed from the result in Figure 8a,c that high ionic conductivity is favorable, but good interfacial contact is more important for the solid electrolyte. Obviously, the liquid electrolyte possesses both advantages.

As discussed above, I_3^- has to be produced via photoelectrochemical reactions. This may influence the power-law results, especially when the system is not in a real steady state. Figure 9 compares the relationship of J_{sc} and radiant power of the electrolyte systems with the addition of I_2 (I_2/LiI = 1:50, molar ratio) in advance. It can be seen that all systems show better linear behavior. Similarly, LiI$(HPN)_4$/15 wt %-nano-SiO_2 shows the highest J_{sc} as in Figure 8. Comparing the J_{sc} value for the same electrolyte system (Figures 8 and 9), we can see that the addition of I_2 in advance is helpful to increase J_{sc}. The results

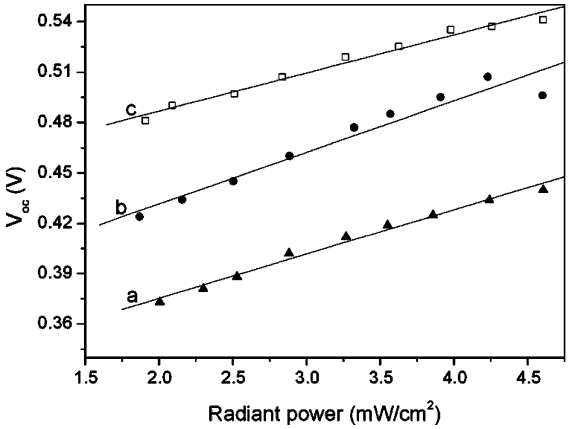

Figure 10. Dependence of V_{oc} of DSSC fabricated with solid electrolyte with and without silica on logarithmic incident power intensity (InP_0): (a) $LiI(HPN)_4$, (b) $LiI(HPN)_4$/20 wt % μm-SiO_2, (c) $LiI(HPN)_4$/15 wt % nm-SiO_2.

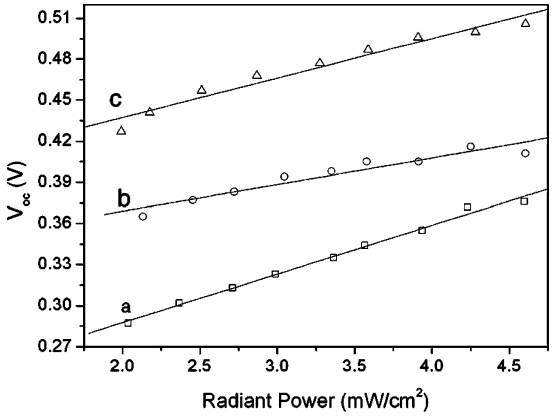

Figure 11. Dependence of V_{oc} of DSSC assembled with solid electrolyte with iodine added (I_2/LiI = 1:50, molar ratio) on the logarithmic radiant power: (a) $LiI(HPN)_4$, (b) $LiI(HPN)_4$/20 wt % μm-SiO_2, (c) $LiI(HPN)_4$/15 wt % nm-SiO_2.

in Figure 8, 9, and 7b indicate that high ionic conductivity and good interfacial contact are both important for the solid electrolyte to achieve high J_{sc}.

The V_{oc} value of DSSC is determined by the difference between energy level for electrons in the TiO_2 electrode and the redox potential of I^-/I_3^- at the counter electrode.[32] The V_{oc} can be increased by continuous injection of electrons from the excited state of the dye to the conduction band of TiO_2. However, this effect is reduced by the recombination of injected electrons with the oxidized state of the dye and/or the oxidized species in the electrolyte (dark current). Since $LiI(HPN)_2$ and $LiI(HPN)_4$ easily form big crystals, it is difficult for the electrolytes to fully penetrate into the pores of the TiO_2 film. As a result, some interface regions of the TiO_2/dye are naked without wetting by the electrolyte. In the absence of the electrolyte, the injected conduction band electrons or electrons at the excited-state dye can be recaptured by the oxidized dye molecules.[33] The dark current increases and V_{oc} decreases. Therefore, good interfacial contact is important to reduce the above dark current. On the other hand, another source of dark current is related to the back reaction of injected electrons from the conduction band of TiO_2 to I_3^- at the electrode/electrolyte interface. It will also decrease V_{oc}. Since the compositions of the electrolytes are the same except the content of silica, this dark current should be equivalent for all systems. Figure 10 illustrates the dependence of V_{oc} on the logarithm of incident light intensity (InP). The response is linear as expected.[34] It can be seen that the highest V_{oc} was achieved at the DSSC fabricated with 15 wt % nano-SiO_2 based electrolyte. Figure 11 shows the relationship of V_{oc} vs InP at DSSC containing iodine (I_2/LiI = 1:50). A similar phenomenon was observed. Comparing the same electrolyte in Figures 10 and 11, we can see that V_{oc} decreases for the same electrolyte with iodine added. The common tendency in Figures 6, 10, and 11 confirms further that the improvement of the interfacial contact is very important for the increase of V_{oc}.

3.4. Pyridine Effect. It has been demonstrated that the rate of the back reaction of injected electrons at TiO_2(CB) with the I_3^- could be reduced by treating the TiO_2 electrode with 4-*tert*-butylpyridine (TBP).[2a] Figure 12 shows the $I-V$ curve of the DSSC fabricated with $LiI(HPN)_4$/20 wt % μm-SiO_2 with (0.3 M TBP, Figure 12d) and without TBP (Figure 12c). The V_{oc} and ff of the DSSC increase from 0.56 to 0.63 V and from 0.53 to 0.56, respectively, after adding TBP into the electrolyte. Although J_{sc} decreases slightly from 12.3 to 11.7 mA/cm^2, the overall conversion efficiency increases from 3.6% to 4.1%. The increase in the V_{oc} is due to the suppression of the recombination of the electrons from the conduction band of TiO_2 to I_3^- by 4-*tert*-butylpyridine.

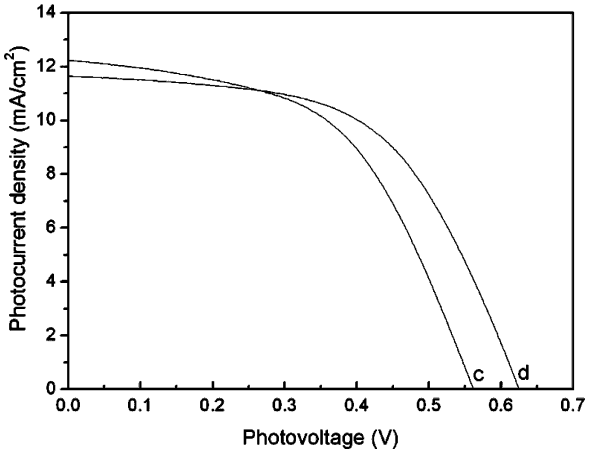

Figure 12. Effect of 4-*tert*-butylpyridine on the performance of DSSC fabricated with composite electrolyte $LiI(HPN)_4$/20 wt % μm-SiO_2 (0.3−2 μm) under the radiant power of 100 mW/cm^2 (illumination area: 0.15 cm^2): (c) without pyridine, (d) containing pyridine (0.3 M).

3.5. Effects of Iodine on the Property of the Electrolytes and the Performance of DSSC. It was found that the conductivity of the electrolyte $LiI(HPN)_4$ or $LiI(HPN)_4$/20 wt % SiO_2 (0.3−2 μm) or $LiI(HPN)_4$/15 wt % SiO_2 (15 nm) decreased with increasing iodine concentration at a concentration range of $0 \le I_2{:}I^- \le 1{:}10$ (molar ratio). This phenomenon is different from the case of ionic liquid electrolytes, where the conductivity increases with increasing iodine concentration due to a Grotthuss exchange mechanism.[35,36] It is supposed that the

(32) Pichot, F.; Gregg, B. A. *J. Phys. Chem. B* **2002**, *104*, 6.
(33) Pelet, S.; Moser, J.-E.; Grätzel, M. *J. Phys. Chem. B* **2000**, *104*, 1791.
(34) Huang, S. H.; SchlichthOrl, G.; Nozik, A. J.; Gratzel, M.; Frank, A. J. *J. Phys. Chem. B* **1997**, *101*, 2576.
(35) Papageorgiou, N.; Athanassov, Y.; Kitamura, T.; Armand, M.; Bonhote, P.; Pettersson, H.; Azam, A.; Grätzel, M. *J. Electrochem. Soc.* **1996**, *143*, 3099.
(36) Kawano, R.; Watanabe, M. *Chem. Commun.* **2003**, 330.

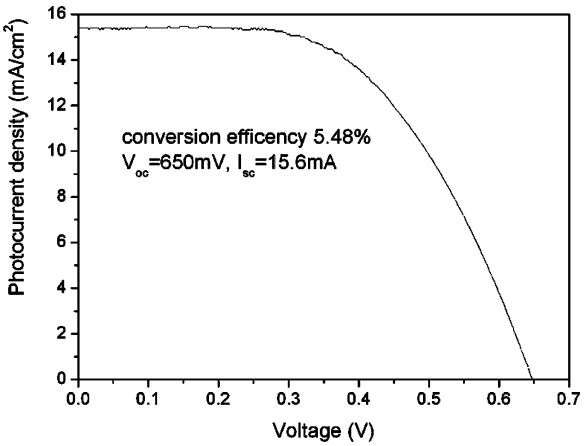

Figure 13. *I*−*V* curve of DSSC assembled with LiI(HPN)$_4$/15 wt % SiO_2 (15 nm) under radiant power of 100 mW/cm^2 (illumination area: 0.15 cm^2).

transport of I_3^- may occur along the grain boundaries in this solid electrolyte. The detailed mechanism needs further clarification in the future. Meanwhile, it was observed that the fill factor of the DSSC changes slightly (0.52−0.56 for LiI(HPN)$_4$/15 wt % SiO_2 (15 nm)) when the ratio of I_2/LiI ranges from 0 to 1:10 (molar ratio). The V_{oc} of the DSSC decreases (Figures 10 and 11) and the J_{sc} increases with increasing iodine concentration at low iodine content in the electrolyte (Figures 8 and 9). However, the J_{sc} decreases if the iodine concentration is beyond a limitation (I_2/LiI = 1:50, molar ratio, in our experiment) due to serious visible light absorbed by I_3^-.[35,37]

3.6. Effect of Nanometer Size Silica on the Performance of DSSC. It was found that the performance of the DSSC fabricated with nanoscale silica based electrolyte could be further enhanced. A conversion efficiency of 5.4% was achieved at DSSC assembled with LiI(HPN)$_4$/15 wt % nano-SiO_2 as solid electrolyte under illumination of 100 mW/cm^2 (Figure 13). The J_{sc} and V_{oc} of the cell reached 15.6 mA/cm^2 and 0.65 V, respectively. Meanwhile, the fact that the conductivity of the electrolyte LiI(HPN)$_4$/15 wt % nano-silica was close to that of the original electrolyte LiI(HPN)$_4$ further suggests that improved interfacial contact of the electrolyte/electrode is the main reason for the increased conversion efficiency of DSSC using a solid electrolyte.

To investigate the stability of the solid electrolyte, the DSSC fabricated with nanocomposite electrolyte LiI(HPN)$_4$/15 wt % SiO_2 (15 nm) was stored in a desiccator without sealing. After one month, the *I*−*V* curve of the DSSC was measured again under 100 mW/cm^2 irradiation (AM 1.5). The result indicated that the light-to-electricity conversion efficiency of the cell reached 70% of the fresh one. This is impossible for the liquid electrolyte. Meanwhile, the morphology of the surface of the TiO_2 film was also detected by SEM (see Figure S4) after one-month storage. It was similar to that of the freshly assembled cell, and no crystalline growth of the electrolyte was observed. The long-term stability will be investigated further in the future in practical devices.

(37) Kubo, W.; Kambe, S.; Nakade, S.; Kitamura, T.; Hanabusa, K.; Wada, Y.; Yanagida, S. *J. Phys. Chem. B* **2003**, *107*, 4374.

A DSSC using a liquid electrolyte shows a high conversion efficiency due to its advantages in ionic conductivity and good interfacial contact between electrolyte and electrode. On the basis of the above study, it is believed that a good solid electrolyte for DSSC should approach these two goals. After controlling particle size, surface polarity, and dispersion situation of the oxide filler in the solid electrolyte, both interfacial contact and conductivity could be improved further.

It has to be mentioned that an organic solvent-based liquid electrolyte was also prepared according to ref 2b and used in DSSC for comparison. The highest energy conversion efficiency was 7.3% by using the same TiO_2 porous films as our solid electrolytes for DSSC. This efficiency is lower than that in ref 2b, which means that the quality of the TiO_2 porous film (porosity, thickness, roughness, etc.) is not optimized.

We believe that the performance of the DSSC based on this series of solid electrolytes can be improved after optimizing the nanocrystalline film and other assembling processes.

4. Summary

A new compound, LiI(HPN)$_2$, is found to possess 3-D transporting paths for iodine and a mono-ion transport feature. These features make LiI(HPN)$_x$ ($2 \le x \le 4$) suitable candidates as solid electrolyte for dye-sensitized solar cells (DSSC). However, the performance of the DSSC assembled with the electrolyte is not satisfactory due to relative low conductivity and poor filling and contact of the electrolyte with the porous TiO_2 electrode. Addition of micrometer-sized and nanosized SiO_2 particles into the solid electrolyte enhanced the conductivity of the electrolyte and improved the interfacial contact between electrode/electrolyte greatly. Consequently, using an optimized composite solid electrolyte system to fabricate DSSC, a light-to-electricity conversion efficiency of 5.4% was achieved under AM 1.5 simulated solar light illumination. The light-to-electricity conversion efficiency of the DSSC stored in a desiccator for one month without sealing reached 70% of the fresh one. Due to the low cost, easy fabrication, and relatively high conversion efficiency, the DSSC based on this new solid-state composite electrolyte is promising for practical applications.

Acknowledgment. The authors appreciate the financial support from the National 863 Program of China (Contract No. 2002AA302403), the National 973 Program (G001CB309503), and the "100-talent" project of Chinese Academy of Sciences. The authors acknowledge Dr. Shi Siqi, Dr. Xu Lifang and Prof. Wang Enge for their valuable theoretical calculation work and Dr. Wu Li for her work in dealing with the single-crystal structure of LiI(HPN)$_2$.

Supporting Information Available: Details of the single-crystal structure and DSC of LiI(HPN)$_2$, XRD and SEM of the LiI(HPN)$_4$ with and without SiO_2, and transport properties of LiI(HPN)$_2$. This information is available free of charge via Internet at http://pubs.acs.org.

JA043268P